Speed Estimators Using Stator Resistance Adaption for Sensorless Induction Motor Drive

Hau Huu VO[1], *Pavel BRANDSTETTER*[2], *Chau Si Thien DONG*[1], *Thinh Cong TRAN*[1]

[1]Faculty of Electrical and Electronics Engineering, Ton Duc Thang University,
19 Nguyen Huu Tho, Dist. 7, Ho Chi Minh City, Vietnam
[2]Department of Electronics, Faculty of Electrical Engineering and Computer Science,
VSB–Technical University of Ostrava, 17. listopadu 15, 708 33 Ostrava, Czech Republic

vohuuhau@tdt.edu.vn, pavel.brandstetter@vsb.cz, dongsithienchau@tdt.edu.vn, trancongthinh@tdt.edu.vn

DOI: 10.15598/aeee.v14i3.1732

Abstract. *The paper describes speed estimators for a speed sensorless induction motor drive with the direct torque and flux control. However, the accuracy of the direct torque control depends on the correct information of the stator resistance, because its value varies with working conditions of the induction motor. Hence, a stator resistance adaptation is necessary. Two techniques were developed for solving this problem: model reference adaptive system based scheme and artificial neural network based scheme. At first, the sensorless control structures of the induction motor drive were implemented in Matlab-Simulink environment. Then, a comparison is done by evaluating the rotor speed difference. The simulation results confirm that speed estimators and adaptation techniques are simple to simulate and experiment. By comparison of both speed estimators and both adaptation techniques, the current based model reference adaptive system estimator with the artificial neural network based adaptation technique gives higher accuracy of the speed estimation.*

Keywords

Artificial neural network, induction motor drive, model reference adaptive system, sensorless control.

1. Introduction

The control and estimation of induction motor drives is almost an unbounded subject, and the technology has been developing very strong in last few decades. The induction motor drive with a cage type of machine has many applications in industry such as pumps and fans, paper and textile mills, subway and locomotive propulsions, electric and hybrid vehicles, machine tools and robotics, home appliances, heat pumps and air conditioners, rolling mills, wind generation systems. These applications often require adjustable speed and wide power range [1] and [2]. The control methods without speed encoder can be classified as follows:

- Methods without machine model: estimators with injection methods and estimators using artificial intelligence such as neural network [3].
- Methods with machine model [4], [5], [6] and [7]: open loop estimators, Model Reference Adaptive System (MRAS) and observers (such as extended Kalman filter, Luenberger observer, sliding mode observer). These methods are simple, but sensitive to variations of parameters of induction motor such as the vector control is very sensitive to variations in the rotor time constant [8].

2. Speed Estimators with Stator Resistance Adaptation

The Direct Torque and Flux control (DTC) has comparable performance with the vector control. In this control scheme, the torque and the stator flux are controlled by selecting voltage space vector of the inverter through a look-up table. The errors between the command torque and stator flux with estimated values will be processed by two hysteresis-band controllers: a flux controller and a torque controller.

The DTC technique has many advantages such as no feedback current control, no traditional Pulse Width

Modulation algorithm, and no vector transformation. However, the DTC is very sensitive to variation of stator resistance.

In general, methods of stator resistance estimation are similar to those utilized for rotor time constant (rotor resistance) estimation and include application of observers, extended Kalman filters, model reference adaptive systems, and artificial intelligence [9]. In this paper, two MRAS-based adaptation mechanisms with two MRAS speed estimators are implemented on MATLAB software: Proportional-Integral (PI) controller and Artificial Neural Network (ANN).

2.1. Reference Frame MRAS

The structure of a reference frame model reference adaptive system (RF-MRAS) with stator resistance adaptation for the rotor speed estimation is shown in Fig. 1. In the reference model, the stator voltages and stator currents are used for obtaining rotor flux vector components. In the adaptive model, these components of the estimated rotor flux vector can be gotten from stator currents together with the exact value of rotor speed.

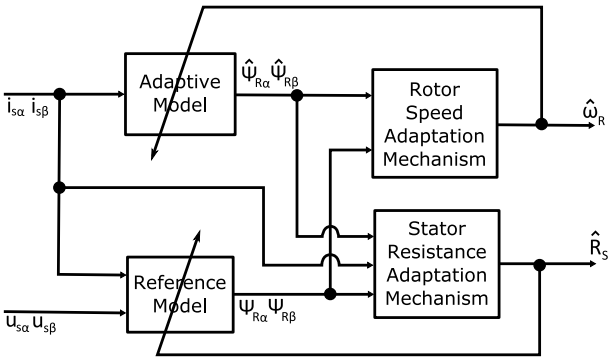

Fig. 1: Structure of RF-MRAS.

The correlative rotor flux vector components from the reference model and the adaptive model will be equal in ideal condition (such as the exact knowledge of stator resistance).

However, the accuracy of this method is decreased because of parameter variations (such as uncertainty of stator resistance or rotor time constant). Thus, for improving the performance of the RF-MRAS scheme, a stator resistance adaptation mechanism (SRAM) is added to update stator resistance.

The outputs of reference model and adaptive model are calculated according to the following equations:

$$\begin{aligned}\psi_{R\alpha} &= \frac{L_r}{L_m}\int\left(u_{s\alpha}-\hat{R}_s i_{s\alpha}\right)dt-\sigma L_s i_{s\alpha},\\ \psi_{R\beta} &= \frac{L_r}{L_m}\int\left(u_{s\beta}-\hat{R}_s i_{s\beta}\right)dt-\sigma L_s i_{s\beta},\end{aligned} \tag{1}$$

$$\begin{aligned}\hat{\psi}_{R\alpha} &= \int\left(\frac{L_m}{T_r}i_{s\alpha}-\frac{1}{T_r}\hat{\psi}_{R\alpha}-\hat{\omega}_r\hat{\psi}_{R\beta}\right)dt,\\ \hat{\psi}_{R\beta} &= \int\left(\frac{L_m}{T_r}i_{s\beta}-\frac{1}{T_r}\hat{\psi}_{R\beta}+\hat{\omega}_r\hat{\psi}_{R\alpha}\right)dt.\end{aligned} \tag{2}$$

Using the Popov's criterion for hyperstability for a globally asymptotically stable system, the rotor speed adaptation mechanism uses the adaptive signal ξ to tune the rotor speed:

$$\begin{aligned}\xi &= \hat{\psi}_{R\alpha}\psi_{R\beta}-\hat{\psi}_{R\beta}\psi_{R\alpha},\\ \hat{\omega}_r &= K_P\xi+K_I\int_0^t\xi dt,\end{aligned} \tag{3}$$

where $K_P > 0$, $K_I > 0$.

2.2. Current Based MRAS

Figure 2 shows the structure of a current-based model reference adaptive system (CB-MRAS) with the stator resistance adaptation for the rotor speed estimation. This MRAS estimator uses stator currents as output quantities of the reference model [7].

The CB-MRAS scheme has one reference model (stator currents of induction motor) and two adaptive models (current model and current estimator).

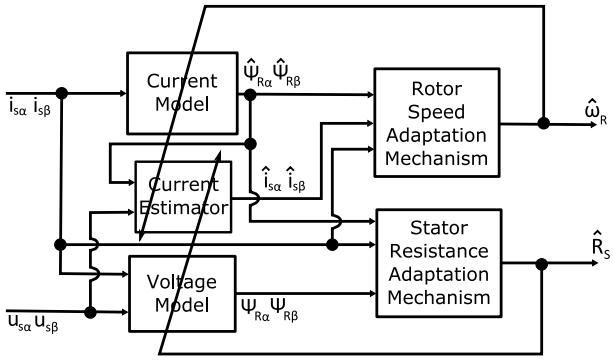

Fig. 2: Structure of CB-MRAS.

The outputs of current model are also described with Eq. (2); the outputs of the current estimator are calculated:

$$\begin{aligned}\hat{i}_{s\alpha} &= \tfrac{1}{T_i}\int\left(K_1u_{s\alpha}+K_2\hat{\psi}_{R\alpha}+K_3\hat{\omega}_R\hat{\psi}_{R\beta}-\hat{i}_{s\alpha}\right)dt,\\ \hat{i}_{s\beta} &= \tfrac{1}{T_i}\int\left(K_1u_{s\beta}+K_2\hat{\psi}_{R\beta}-K_3\hat{\omega}_R\hat{\psi}_{R\alpha}-\hat{i}_{s\beta}\right)dt,\end{aligned} \tag{4}$$

where:

$$\begin{aligned}K_1 &= \frac{L_r}{C_1L_m},\ K_2=\frac{L_m}{C_1(L_r\hat{R}_sT_r+L_m^2)},\\ K_3 &= \frac{1}{C_1},\ T_i=\frac{L_sL_r-L_m^2}{C_1L_m},\ C_1=\frac{L_r\hat{R}_s}{L_m}+\frac{L_m}{T_r}.\end{aligned} \tag{5}$$

As in RF-MRAS scheme, stator resistance is also updated by a similar SRAM. Besides that, the voltage

model is supplemented to obtain components of the rotor flux vector according to Eq. (1). The following equation is used by rotor speed adaptation mechanism for obtaining the rotor speed:

$$\begin{aligned} \xi &= \left(i_{s\alpha} - \hat{i}_{s\alpha}\right)\hat{\psi}_{R\beta} - \left(i_{s\beta} - \hat{i}_{s\beta}\right)\hat{\psi}_{R\alpha}, \\ \hat{\omega}_r &= K_P\xi + K_I\int_0^t \xi dt, \end{aligned} \tag{6}$$

where $K_{PRs} > 0$, $K_{IRs} > 0$.

2.3. MRAS-Based SRAMs

The inputs of the stator resistance adaptation mechanisms are outputs of reference and adaptive models for RF-MRAS (see Fig. 1), or current and voltage models for CB-MRAS (see Fig. 2). The adaptive signal, derived from the error between two models, is used to estimate stator resistance by PI adaptation mechanism:

$$\begin{aligned} \xi_{Rs} &= \left(\psi_{R\alpha} - \hat{\psi}_{R\alpha}\right)i_{s\alpha} + \left(\psi_{R\beta} - \hat{\psi}_{R\beta}\right)i_{s\beta}, \\ \hat{R}_s &= K_{PRs}\xi_{Rs} + K_{IRs}\int_0^t \xi_{Rs}dt, \end{aligned} \tag{7}$$

where $K_{PRs} > 0$, $K_{IRs} > 0$.

Equation (7) is discretized into the following equation with sampling period T_s:

$$\begin{aligned} \hat{R}_s(k) &= \hat{R}_s(k-1) + K_{PRs}\xi_{Rs}(k) \\ &+ K_{IRs}T_s\frac{\xi_{Rs}(k) + \xi_{Rs}(k-1)}{2}. \end{aligned} \tag{8}$$

Equation (9) is produced by generalizing Eq. (8):

$$\hat{R}_s(k) = f\left(\xi_{Rs}(k), \xi_{Rs}(k-1), \hat{R}_s(k-1)\right). \tag{9}$$

Based on Eq. (9), an ANN adaptation mechanism is proposed as in Fig. 3.

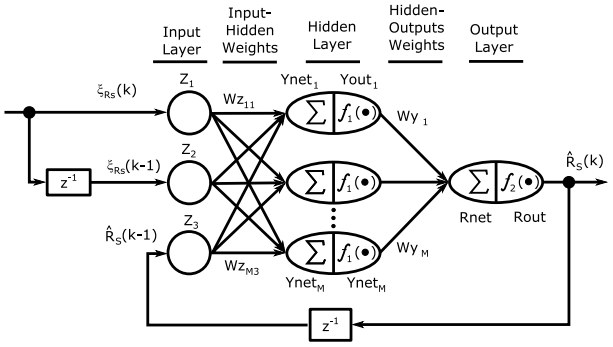

Fig. 3: Structure of ANN adaptation mechanism.

This feed-forward neural network has three layers: one input layer with three neurons (three parameters of f), one hidden layer with M neuron(s) ($3M$ input-hidden weights and M hidden-output weights), and one output layer with one neuron (estimated value of stator resistance). The signal propagation process from the neurons of input layer to the neuron of output layer is done:

$$\begin{aligned} Ynet_j(k) &= \sum_{i=1}^{3} Wz_{ji}(k)Z_i(k), \\ Yout_j(k) &= f_1(Ynet_j(k)), \\ Rnet(k) &= \sum_{j=1}^{M} Wy_j(k)Yout_j(k), \\ \hat{R}_s(k) &= Rout(k) = f_2(Rnet(k)), \end{aligned} \tag{10}$$

where:

$$\begin{aligned} Z_1(k) &= \xi_{Rs}(k), \\ Z_2(k) &= \xi_{Rs}(k-1), \\ Z_3(k) &= \hat{R}_s(k-1), \\ f_1(x) &= \frac{2}{1+e^{-x}} - 1, \\ f_2(x) &= \frac{\hat{R}_s}{1+e^{-x}} + 0.5R_s. \end{aligned} \tag{11}$$

Function f_2 is chosen with assumption that $\hat{R}_s \in (0.5R_s; 1.5R_s)$. The cost function E is minimized by updating weights of ANN according to Eq. (12):

$$\begin{aligned} E(k) &= \frac{1}{2}\left[\bar{R}_s - \hat{R}_s(k)\right]^2, \\ Wy_j(k+1) &= Wy_j(k) - \eta(k)\cdot\frac{\partial E(k)}{\partial Wy_j(k)}, \\ Wz_{ji}(k+1) &= Wz_{ji}(k) - \eta(k)\cdot\frac{\partial E(k)}{\partial Wz_{ji}(k)} \end{aligned} \tag{12}$$

where $\eta(k) > 0$ is the learning rate, and:

$$\begin{aligned} \frac{\partial E(k)}{\partial Wy_j(k)} &= C_2C_3Yout_j(k), \\ \frac{\partial E(k)}{\partial Wz_{ji}(k)} &= \frac{C_2C_3Wy_j(k)\left(1-Yout_j^2(k)\right)\cdot Z_i(k)}{2}, \\ C_2 &= -(\bar{R}_s - \hat{R}_s(k)), \\ C_3 &= \frac{(Rout(k)-0.5R_s)(1.5R_s-Rout(k))}{R_s}. \end{aligned} \tag{13}$$

The term C_2 is unknown. Assume that $\zeta_{Rs}(k) \approx \zeta_{Rs}(k-1)$, based on Eq. (8), this term can be replaced with the term $\zeta_{Rs}(k)$, and for faster convergence $C_2 = |\zeta_{Rs}(k)|\zeta_{Rs}(k)$. In this network, learning rate is also adapted by the following rule:

$$\begin{aligned} \Delta E(k) &= Z_1^2(k) - Z_2^2(k), \\ \eta(k+1) &= \begin{cases} \eta(k) + 0.005, & \text{if } \Delta E(k) < 0, \\ \eta(k) - 0.005\eta(k), & \text{if } \Delta E(k) > 0, \\ \eta(k), & \text{otherwise}, \end{cases} \end{aligned} \tag{14}$$

where:

$$\Delta E(k) = Z_1^2(k) - Z_2^2(k). \tag{15}$$

3. Simulation Results

The designed control algorithms were simulated in sensorless control structure of the induction motor drive

using Matlab-Simulink. Time courses of important quantities were obtained from the control structure with two MRAS speed estimators and two SRAMs at the jump of the load torque $T_L = 2$ Nm (see Fig. 4). The results in Fig. 5, Fig. 6, Fig. 7, Fig. 8, Fig. 9, Fig. 10 are done with $\bar{R}_S = 1.2R_S$, $M = 1$ and initial values of weights in ANN are random real number in range $(-10^{-3}, +10^{-3})$. Table 1 and Tab. 2 shows a comparison in maximum value of absolute of speed difference (MSD), steady-state error of estimated stator resistance (ESSR), maximum value of estimated stator resistance (MESR), root mean square error between reference torque and motor torque (RMSET).

Tab. 1: Comparison with RF-MRAS speed estimator.

Quantity	PI	ANN with M-neuron hidden layer				
		1	2	3	4	5
MSD [rpm]	3.76	3.41	3.41	3.4	3.4	3.4
ESSR $[\times 10^{-4} R_s]$	75	64.1	41.3	28.4	24.6	18.2
MESR $[\times R_s]$	1.28	1.48	1.49	1.49	1.49	1.49
RMSET $[N_m]$	0.27	0.27	0.27	0.27	0.26	0.27

Tab. 2: Comparison with CB-MRAS speed estimator.

Quantity	PI	ANN with M-neuron hidden layer				
		1	2	3	4	5
MSD [rpm]	1	0.54	0.97	0.77	0.74	0.85
ESSR $[\times 10^{-4} R_s]$	2	0.33	1.2	0.14	0.12	0.1
MESR $[\times R_s]$	1.28	1.48	1.49	1.49	1.49	1.5
RMSET $[N_m]$	0.26	0.26	0.26	0.26	0.26	0.26

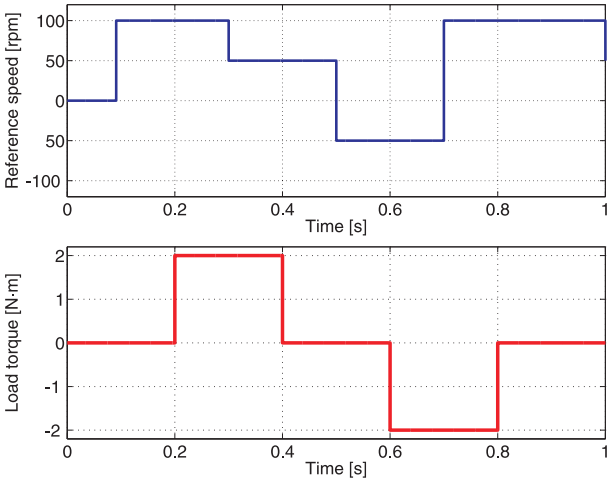

Fig. 4: Reference speed and load torque.

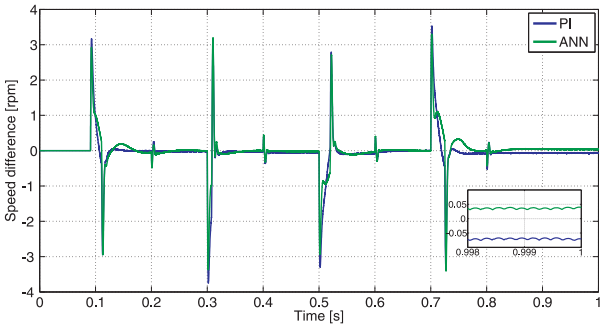

Fig. 5: RF-MRAS with PI (blue) and ANN (green) adaptation mechanisms, difference between real speed and estimated speed.

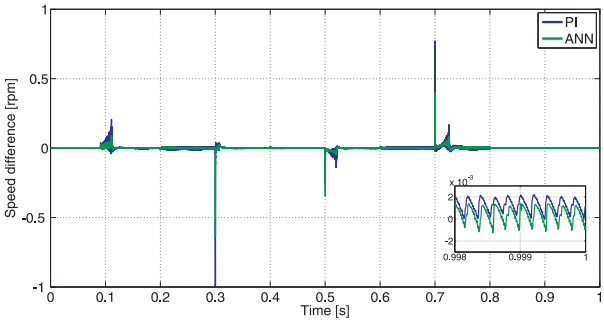

Fig. 6: CB-MRAS with PI (blue) and ANN (green) adaptation mechanisms, difference between real speed and estimated speed.

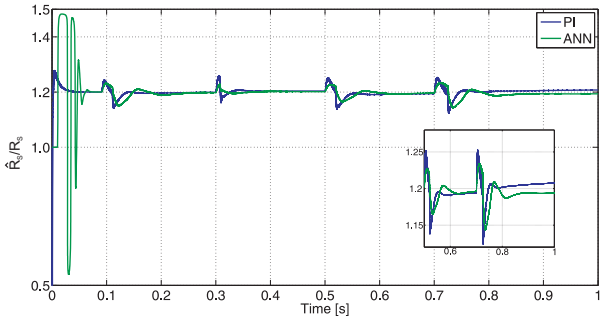

Fig. 7: RF-MRAS with PI (blue) and ANN (green) adaptation mechanisms, ratio between estimated value and known value of stator resistance.

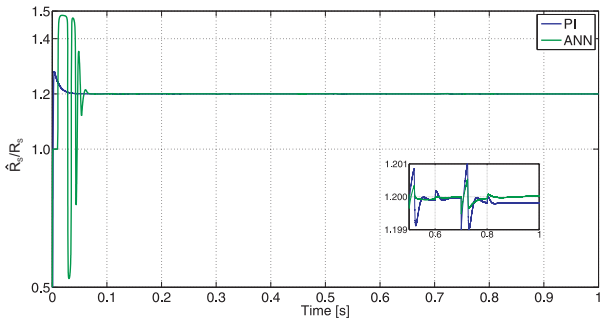

Fig. 8: CB-MRAS with PI (blue) and ANN (green) adaptation mechanisms, ratio between estimated value and known value of stator resistance speed.

The first rows of Tab. 1 and Tab. 2, Fig. 5 and Fig. 6 show that ANN mechanism gives smaller MSD than PI mechanism, MSD of CB-MRAS is smaller than that of RF-MRAS, and CB-MRAS with ANN mechanism (with only one-neuron in hidden layer) produces the smallest MSD. PI mechanism gives larger ESSR and smaller MESR (smaller overshoot) than ANN one does, and approximate-zero ESSR belongs to CB-MRAS with ANN mechanism as shown in Fig. 7 and Fig. 8 and the second and third rows of Tab. 1 and Tab. 2.

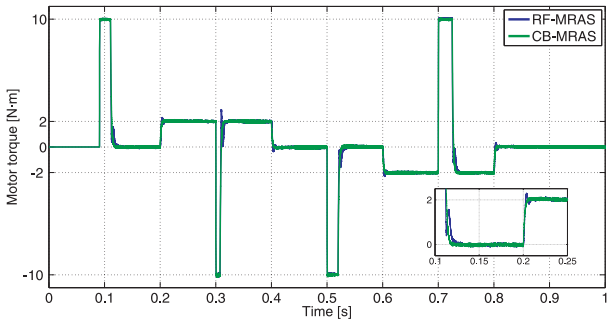

Fig. 9: RF-MRAS (blue) and CB-MRAS (green) with PI adaptation mechanism, motor torque.

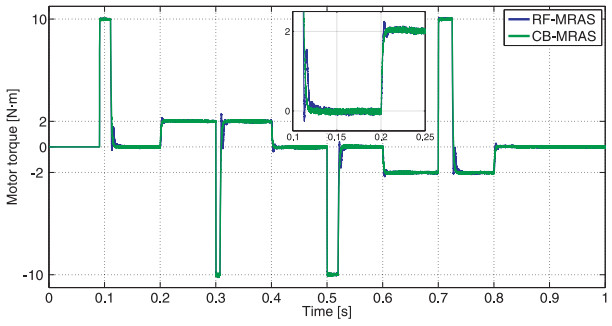

Fig. 10: RF-MRAS (blue) and CB-MRAS (green) with ANN adaptation mechanism, motor torque.

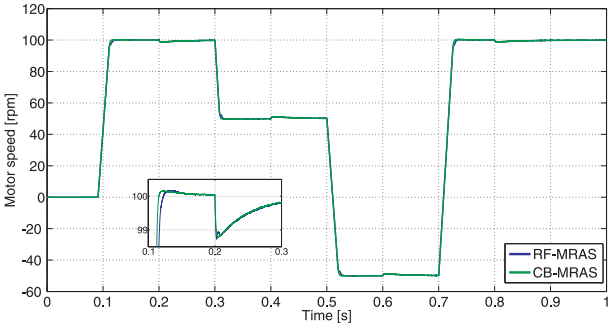

Fig. 11: RF-MRAS (blue) and CB-MRAS (green) with PI adaptation mechanism, motor speed.

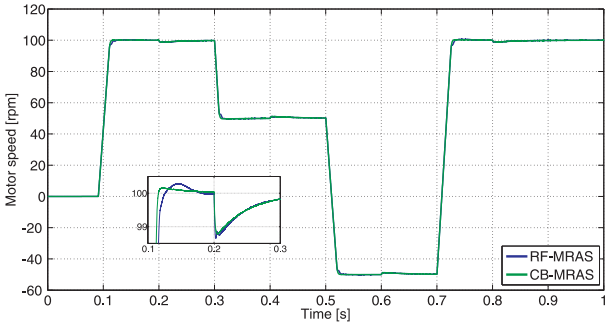

Fig. 12: RF-MRAS (blue) and CB-MRAS (green) with ANN adaptation mechanism, motor speed.

RMSET of both MRAS schemes with two SRAMs are almost equal (the fourth rows of Tab. 1 and Tab. 2), but motor torque and motor speed time courses of CB-MRAS are smoother than those of RF-MRAS (Fig. 9, Fig. 10, Fig. 11, Fig. 12).

4. Conclusion

The MRAS-based speed sensorless induction motor drive with the direct torque control was presented in the paper. The DTC drive with two MRAS estimators together with two MRAS-based SRAMs gave good dynamic responses and the estimation of the rotor speed was good in steady state and also in transient state. The CB-MRAS scheme gave higher accuracy of the rotor speed estimation than the RF-MRAS scheme, and the ANN mechanism gave higher accuracy of the stator resistance adaptation than the PI mechanism. However, response of the stator resistance estimation for ANN adaptation mechanism at beginning times is not good and should be improved. The CB-MRAS estimator with both MRAS-based SRAMs could be used for speed estimation with the uncertainty of stator resistance without speed encoder in the control system with digital signal processor. The simple MRAS-based ANN adaptation mechanism with only one-neuron hidden layer can be applied for estimating other parameters of induction motor.

Acknowledgment

The paper was supported by the projects: Center for Intelligent Drives and Advanced Machine Control (CIDAM) project, reg. no. TE02000103 funded by the Technology Agency of the Czech Republic, project reg. no. SP2016/83 funded by the Student Grant Competition of VSB–Technical University of Ostrava.

References

[1] HOLTZ, J. Sensorless Control of Induction Motor Drives. *Proceedings of the IEEE.* 2002, vol. 90, iss. 8, pp. 1359–1394. ISSN 0018-9219. DOI: 10.1109/JPROC.2002.800726.

[2] VAS, P. *Sensorless Vector and Direct Torque Control.* Oxford University Press, 1998. ISBN 978-0198564652.

[3] GADOUE, S. M., D. GIAOURIS and J. W. FINCH. Sensorless Control of Induction Motor Drives at Very Low and Zero Speeds Using Neural Network Flux Observers. *IEEE Transactions on Industrial Electronics.* 2009, vol. 56, iss. 8, pp. 3029–3039. ISSN 0278-0046. DOI: 10.1109/TIE.2009.2024665.

[4] SUTNAR, Z., Z. PEROUTKA and M. RODIC. Comparison of sliding mode observer and extended Kalman filter for sensorless DTC controlled induction motor drive. In: *14th International Power Electronics and Motion Control Conference (EPE/PEMC).* Ohrid: IEEE, 2010, pp. 55–62. ISBN 978-1-4244-7856-9. DOI: 10.1109/EPE PEMC.2010.5606844.

[5] LASCU, C., I. BOLDEA and F. BLAABJERG. Comparative Study of Adaptive and Inherently Sensorless Observers for Variable-Speed Induction-Motor Drives. *IEEE Transactions on Industrial Electronics.* 2006, vol. 53, iss. 1, pp. 57–65. ISSN 0278-0046. DOI: 10.1109/TIE.2005.862314.

[6] GACHO, J. and M. ZALMAN. IM Based Speed Servodrive with Luenberger Observer. *Journal of Electrical Engineering.* 2010, vol. 61, iss. 3, pp. 149–156. ISSN 1335-3632. DOI: 10.2478/v10187-011-0021-8.

[7] ORLOWSKA-KOWALSKA, T. and M. DYBKOWSKI. Stator-Current-Based MRAS Estimator for a Wide Range Speed-Sensorless Induction-Motor Drive. *IEEE Transactions on Industrial Electronics.* 2010, vol. 57, iss. 4, pp. 1296–1308. ISSN 0278-0046. DOI: 10.1109/TIE.2009.2031134.

[8] BRANDSTETTER, P., P. CHLEBIS, P. PALACKY and O. SKUTA. Application of RBF Network in Rotor Time Constant Adaptation. *Electronics and Electrical Engineering.* 2011, vol. 113, iss. 7, pp. 21–26. ISSN 1392-1215. DOI: 10.5755/j01.eee.113.7.606.

[9] TOLIYAT, H. A., E. LEVI and M. RAINA. A Review of RFO Induction Motor Parameter Estimation Techniques. *IEEE Transactions on Energy Conversion.* 2003, vol. 18, iss. 2, pp. 271–283. ISSN 0885-8969. DOI: 10.1109/TEC.2003.811719.

About Authors

Hau Huu VO was born in Binh Thuan, Vietnam. He received his M.Sc. degree in Automation Engineering from Ho Chi Minh City of Technology, Vietnam in 2009. His research interests include robotics, control theory and modern control methods of electrical drives.

Pavel BRANDSTETTER was born in Ostrava, Czech Republic. He received his M.Sc. and Ph.D. degrees in Electrical Engineering from Brno University of Technology, Czech Republic, in 1979 and 1987, respectively. He is currently a full professor in electrical machines, apparatus and drives at Department of Electronics, VSB–Technical University of Ostrava. His current research interests are modern control methods of electrical drives, for example sensorless control of AC drives, applications of soft computing methods in control of AC drives.

Chau Si Thien DONG was born in Ho Chi Minh City, Vietnam. She received her M.Sc. degree in Automatic Control from Ho Chi Minh City of Technology, Vietnam in 2004. Her research interests include nonlinear control, adaptive control, robust control, neural network and modern control methods of electrical drives.

Thinh Cong TRAN was born in Da Nang City, Vietnam. He received his M.Sc. degree in Electrical and Electronic Engineering from Ho Chi Minh City of Technology, Vietnam in 1998. His research interests include microcontroller systems and modern control methods of electrical drives.

Appendix: Induction Motor Drive Quantities and Parameters

- $u_{s\alpha}$, $u_{R\beta}$, $i_{s\alpha}$, $i_{s\beta}$, $\hat{i}_{s\alpha}$, $\hat{i}_{s\beta}$, $\psi_{R\alpha}$, $\psi_{R\beta}$, $\hat{\psi}_{R\alpha}$, $\hat{\psi}_{R\beta}$: α, β components of stator voltage vector, stator current vector, estimated stator current vector, rotor flux vector, estimated rotor flux vector,
- ω_r, $\hat{\omega}_r$, T_e, T_L: rotor speed, estimated rotor speed, motor torque, load torque,
- R_s: stator resistance value ($R_s = 1.115\ \Omega$),

- R_r: rotor resistance ($R_r = 1.083\ \Omega$),
- $\bar{R}_s, R_s$: real value and estimated value of stator resistance,
- L_m, L_s, L_r: magnetizing inductance ($L_m = 0.2037$ H), stator inductance ($L_s = 0.2097$ H), rotor inductance ($L_r = 0.2097$ H),
- T_r, J, σ, p: rotor time constant ($T_r = 0.1936$ s), moment of inertia ($J = 0.02$ kg·m^2), total leakage constant ($\sigma = 0.0562$), number of pole pairs ($p = 2$),
- ζ, K_P, K_I: adaptive signal, proportional coefficient ($K_P = 2000$), integral coefficient ($K_I = 1000000$) of MRAS speed estimators,
- ζ_{Rs}, K_{PRs}, K_{IRs}: adaptive signal, proportional coefficient ($K_{PRs} = 10$), integral coefficient ($K_{IRs} = 1000$) of stator resistance adaptation mechanisms.